

Dynamic Detection of Transmission Line Outages Using Hidden Markov Models

Qingqing Huang, Leilai Shao, Na Li

Abstract—In this paper, we study the problem of detecting transmission line outages in power grids. We model the time series of power network measurements as a Hidden Markov process, and formulate the line outage detection problem as an inference problem. Due to the physical nature of the line failure dynamics, the transition probabilities for the Hidden Markov Model are sparse. Taking advantage of this fact, we further propose an approximate inference algorithm using particle filters, which takes in the times series of power network measurements and produces a probabilistic estimation of the status of the transmission lines in real time. We then assess the performance of the proposed algorithm with case studies. We show that it outperforms the conventional static line outage detection algorithms, and is robust to both measurement noise and model parameter errors.

Index Terms—Fault diagnosis, cascading failures, transmission networks, inference.

I. INTRODUCTION

Fault detection and diagnosis play important roles in control and protection for many systems [1], [2]. In this paper, we study the problem of detecting transmission line outages in power networks. Transmission lines form a vital part of the power grid, as they provide the means to transfer electric power from power plants to end users. Unexpected events, such as sudden changes in power generations or loads, a breaker failure, a tree fall, or a lightning strike, can make the transmission lines inoperative. Outage, namely a transmission line being disconnected from the grid, is one of the most common faults. Moreover, the outage of a single transmission line, if not detected and treated quickly, may cascade into the breakdown of multiple lines in a few minutes, and eventually lead to a costly grid-wide outage in less than an hour [3].

Transmission protection systems are designed to identify the locations of faults and to isolate the faulted parts from the rest of the grid. One of the key requirements for the protection system is to detect the faults promptly and accurately. However, due to the large scale of power grids, the highly nonlinear system dynamics, and the limited and noisy power system measurements, fault diagnosis for transmission line failures remains as a challenging problem.

The problem of detecting which transmission lines are possibly disconnected from the grid is typically formulated as various forms of static hypothesis testing / optimization problem. Here, by “static” we refer to that it is usually assumed that the interconnected grid has reached a stable post outage event state, and remains unchanged there. To

identify the line failures based on the readings from phasor measurement units (PMUs), the network topology that offers the minimum fitting error is used as an estimator for the transmission line status. In order to bypass the combinatorial complexity, in [4], [5], the authors applied compressed sensing inspired techniques to convexify the problem. However, these approach all overlook the dynamic process of cascading failure in the transmission networks, which information we incorporate in the proposed algorithm to improve the performance: both in terms of accuracy of estimation of line outages, and of indistinguishable states based on static measurements.

In this paper, we focus on identifying the location and timing of the line outage based on sequences of power system measurements, for example readings from supervisory control and data acquisition (SCADA) system and/or PMU readings. We model the evolution of the transmission line status as a Markov chain which is not directly observable. The power system measurements are thus modeled as the output process of a Hidden Markov Model (HMM). We formulate the problem of line outage detection as an HMM inference problem, i.e. estimating the hidden state based on the observed output process. Due to the physical nature of the line failure dynamics, the transition probabilities are sparse. Taking advantage of this fact, we propose an approximate inference algorithm using particle filters. The proposed algorithm can efficiently locate the line failures and backtrack the cascading failure path over time. We show with numerical case studies that the proposed algorithm is more robust to the measurements noise, can accurately detect some faults which the static algorithm is not able to distinguish, and is associated with a low computational complexity.

In this paper we adopt the AC power flow model and a probabilistic line failure model in the system modeling. However we expect that the general ideas can be applied to more complicated and realistic models, and the benefits described above will remain.

II. PRELIMINARIES

A. AC Power Flow Model

We consider a transmission network consisting of N buses denoted by $\mathcal{N} = \{1, 2, \dots, N\}$ and E transmission lines denoted by $\mathcal{E} = \{1, 2, \dots, E\}$. We use $n \in \mathcal{N}$ to index the bus n and $e \in \mathcal{E}$ to index the transmission line e . We also refer a line e as mn where $m \in \mathcal{N}$ and $n \in \mathcal{N}$ are the two buses it connects. For each bus m , let \mathcal{N}_m denote all of the buses that it is connected to. As a default, we assume $m \notin \mathcal{N}_m$.

First, we derive the bus admittance matrix from the equivalent π model [4]. For each line $mn \in \mathcal{E}$, denote the series admittance by y_{mn} and the total charging susceptance by $b_{c,mn}$. For each bus m , denote the shunt susceptance by

Q. Huang is with the Laboratory of Information and Decision Systems, Massachusetts Institute of Technology, Cambridge, MA 02139, USA (Email: qqh@mit.edu).

L. Shao is with the Very Large Scaled Integrated Circuits Institution, Zhejiang University, Hangzhou, 310027, China (Email:llshao_vlsi@zju.edu.cn).

N. Li is with the school of Engineering and Applied Sciences, Harvard University, Cambridge, MA, 02138, USA (Email: nali@seas.harvard.edu).

$b_{s,mm}$ and let $y_{mm} := j(b_{s,mm} + \sum_{n \in \mathcal{N}_m} b_{c,mn}/2)$. We define the bus admittance matrix $\mathbf{Y} = \mathbf{G} + j\mathbf{B}$ such that the diagonal entries $\mathbf{Y}_{mm} = \sum_{n' \in \mathcal{N}_m} y_{mn'} + y_{mm}$ and the off-diagonal entries $\mathbf{Y}_{mn} = -y_{mn}$ for $n \in \mathcal{N}_m$. Then, the polar presentation of the power flow equations yields is given by:

$$\mathbf{P}_m = \sum_{n \in \mathcal{N}} V_m V_n (G_{mn} \cos \theta_{mn} + B_{mn} \sin \theta_{mn}), \quad (1)$$

$$\mathbf{Q}_m = \sum_{n \in \mathcal{N}} V_m V_n (G_{mn} \sin \theta_{mn} - B_{mn} \cos \theta_{mn}), \quad (2)$$

where V_m denotes the voltage magnitude at bus m , $\theta_{mn} := \theta_m - \theta_n$ denotes the phase difference on transmission line mn and $\mathcal{S}_m := \mathbf{P}_m + j\mathbf{Q}_m$ denotes the power injection at bus m .

Given the system power injection profile \mathcal{S} and system admittance matrix \mathbf{Y} , the complex voltages $\mathcal{V}_m := V_m e^{j\theta}$ can be solved through (1) – (2), as a standard AC power flow problem [6]. Invoking Ohm's and Kirchoff's laws, the complex current \mathcal{I}_{mn} and power flow on transmission line mn are given by:

$$\mathcal{I}_{mn} = (jb_{c,mn}/2 + y_{mn})\mathcal{V}_m - y_{mn}\mathcal{V}_n, \quad (3)$$

$$\mathcal{F}_{mn} = \mathcal{V}_m \mathcal{I}_{mn}^*. \quad (4)$$

B. Hidden Markov Model

An HMM is a statistical model in which the underlying system is assumed to be a Markov process with unobserved (hidden) states [7]. As illustrated in In this paper, we will focus on stationary HMMs. We use \mathbf{h}_t to denote the hidden state and use random variable \mathbf{z}_t denote the observation at time t . The hidden states form a stationary Markov process with the state transition probabilities given by $\mathbb{P}(\mathbf{h}_t | \mathbf{h}_{t-1})$; and conditional on the hidden state at time t , the observation is independent of all other variables and follows the conditional probability distribution $\mathbb{P}(\mathbf{z}_t | \mathbf{h}_t)$.

III. SYSTEM MODEL

In this section, we formulate the fault diagnosis problem as an HMM inference problem. We first introduce the HMM for the fault diagnosis system.

A. Hidden states and the transition probabilities

We denote the line status configuration by a vector $\mathbf{l} \triangleq (l_1, \dots, l_E)$ assuming values in the set $\{0, 1\}^E$, where $l_e = 0$ indicates that line e is disconnected and $l_e = 1$ indicates that line e is connected. Let $\Gamma(\mathbf{l}) = \{e \in \mathcal{E} : l_e = 1\}$ denote the set of good lines for the network configuration \mathbf{l} . We denote the line status at time t by \mathbf{l}_t and $\Gamma_t = \Gamma(\mathbf{l}_t)$. The objective of fault diagnosis considered in this paper is to infer about \mathbf{l}_t over time. Note that the line status \mathbf{l}_t and the power injection profile \mathcal{S}_t are not directly observed, and we define the hidden state of the system to be: $\mathbf{h}_t = (\mathbf{l}_t, \mathcal{S}_t)$.

Given a system power injection profile \mathcal{S}_t and a system structure topology \mathbf{l}_t , the voltages \mathcal{V}_t , the currents \mathcal{I}_t and the power flows \mathcal{F}_t can be solved based on the AC power flow model with equation (1)–(2)–(3)–(4). Therefore, We write the corresponding \mathcal{V}_t , \mathcal{I}_t and \mathcal{F}_t as $\mathcal{V}_t(\mathbf{h}_t)$, $\mathcal{I}_t(\mathbf{h}_t)$ and $\mathcal{F}_t(\mathbf{h}_t)$. At time t , if the power flow $\mathcal{F}_{e,t}$ on a line e exceeds its thermal limit \bar{F}_e , the line will trip or disconnect with a very high probability. Once a line or multiple lines

trip, the power injection \mathcal{S}_t of the system will change or stay the same according to the system regulation rules; and then based on the new network topology and the possibly new power injection profile, the voltages, currents and the power flows update passively. This failing process continues until the system stabilizes itself or a system-wide outage occurs. Therefore, we model the transition probability as below:

$$\begin{aligned} \mathbb{P}(\mathbf{h}_{t+1} | \mathbf{h}_t) &= \mathbb{P}(\mathbf{l}_{t+1} | \mathbf{h}_t) \mathbb{P}(\mathcal{S}_{t+1} | \mathbf{l}_{t+1}, \mathcal{S}_t) \\ &= \mathbb{P}(\mathbf{l}_{t+1} | \mathcal{F}_t(\mathbf{h}_t)) \mathbb{P}(\mathcal{S}_{t+1} | \mathbf{l}_{t+1}, \mathcal{S}_t). \end{aligned} \quad (5)$$

Note that there are two components in this transition probability. The first one corresponds to the line failure model which depends on the power flow profile $\mathcal{F}_t(\mathbf{h}_t)$; the second component captures the power re-dispatch policies and the stochastic nature of the power injections, such as the time varying generations and consumptions.

1) *Line Failure Model*: We first derive the probabilistic line failure model based on the widely used failure model introduced in [8], [9]. We assume that once a line fails, it will not recover during the time span we consider. We use a probabilistic model to capture the power system dynamics during the cascading failure.

Considering all the uncertainties, we model the outage of a overloaded line by an independent probability, which is a function of the power flow and the line capacity. In particular, given the power flow $\mathcal{F}_{e,t}$, the event that an operating transmission line ($l_{e,t} = 1$) fails in the next time slot ($l_{e,t+1} = 0$) happens with an independent probability:

$$q_{e,t} = \begin{cases} g_1\left(\frac{|\mathcal{F}_{e,t}|}{\bar{F}_e}\right) & \text{if } |\mathcal{F}_{e,t}| < \bar{F}_e \\ g_2\left(\frac{|\mathcal{F}_{e,t}|}{\bar{F}_e}\right) & \text{if } |\mathcal{F}_{e,t}| \geq \bar{F}_e \end{cases}, \quad (6)$$

where the initial failure probability $g_1(\cdot)$ and overloading failure probability $g_2(\cdot)$ are non-decreasing functions. Therefore, given the power flow profile \mathcal{F}_t , the line failures are independent events, and the probability $\mathbb{P}(\mathbf{l}_{t+1} | \mathcal{F}_t(\mathbf{h}_t))$ is given by:

$$\mathbb{P}(\mathbf{l}_{t+1} | \mathcal{F}_t) = \prod_{e \in \Gamma_t \setminus \Gamma_{t+1}} q_{e,t} \prod_{e' \in \Gamma_{t+1}} (1 - q_{e',t}). \quad (7)$$

The work in [10] provided analysis and simulations of the transient response of transmission lines, which can be used to justify the above abstract modeling of the line failure process.

Remark 1 (Sparsity): A remarkable feature of the failure model is the sparsity of the transition probabilities $\mathbb{P}(\mathbf{h}_{t+1} | \mathcal{F}_t)$, in the sense that with a moderate system loading profile, only a small portion of the transmission lines are overloaded during the initial stages of the failure process. Moreover, with high probability, the new failures $\Gamma_t \setminus \Gamma_{t+1}$ only occur on a small subset of the overloaded lines. These two facts result in a sparse transition probability $\mathbb{P}(\mathbf{l}_{t+1} | \mathbf{h}_t)$.

2) *Stochastic Power Injection Policy*: On one hand, the power injection profile \mathcal{S}_{t+1} depends on the system regulation rules¹. On the other hand, the power injection is stochastic per se due to the time varying supply and demand. These two facts are captured by the conditional probability of $\mathbb{P}(\mathcal{S}_{t+1} | \mathbf{l}_{t+1}, \mathcal{S}_t)$, which can be learned from the historical

¹Note that the system is equipped with various automatic control and protection mechanisms in response to disturbances and/or emergencies. Thus, even if the system operator is not aware of the line failures, there would be automatic response on the generations and loads.

data of the power injection time series, as well as be derived based on the knowledge of the protection mechanisms.

B. Observation and the observation probabilities

There are typically four physical quantities that can be measured in the power system [11]. The conventional SCADA system measures the magnitude of power injection on selected buses, and magnitude of power flow on selected lines; whereas the new technology of PMU can measure the complex voltages on selected buses and the complex current on selected adjacent transmission lines. Throughout this paper, we only consider the PMU measurements. However, the proposed algorithm is generic and can be applied to the setup with other measurements.

At time t , we denote the voltage magnitude at bus n as \mathbf{V}_t^n and the phase angle at bus n as $\boldsymbol{\theta}_t^n$. Similarly, we denote the current magnitude at the line e as \mathbf{I}_t^e and the phase angle difference at the line e as $\boldsymbol{\theta}_t^e$. Denote the subset of buses and the subset of lines where we have the PMU measurements as $\mathcal{N}^o \subseteq \mathcal{N}$ and $\mathcal{E}^o \subseteq \mathcal{E}$. Due to timing misalignment, instrumentation inaccuracy, and modeling uncertainties, the measurements are noisy. We assume the following independent additive noise model of the PMU readings:

$$\tilde{\mathbf{V}}_t^n = \mathbf{V}_t^n + \boldsymbol{\epsilon}_t^n, \quad \forall n \in \mathcal{N}^o, \quad (8)$$

$$\tilde{\boldsymbol{\theta}}_t^n = \boldsymbol{\theta}_t^n + \boldsymbol{\varepsilon}_t^n, \quad \forall n \in \mathcal{N}^o, \quad (9)$$

$$\tilde{\mathbf{I}}_t^e = \mathbf{I}_t^e + \boldsymbol{\eta}_t^e, \quad \forall e \in \mathcal{E}^o, \quad (10)$$

$$\tilde{\boldsymbol{\theta}}_t^e = \boldsymbol{\theta}_t^e + \boldsymbol{\zeta}_t^e, \quad \forall e \in \mathcal{E}^o, \quad (11)$$

where $\epsilon_t^n \sim \mathcal{N}(0, \sigma_\epsilon^2)$, $\varepsilon_t^n \sim \mathcal{N}(0, \sigma_\varepsilon^2)$, $\eta_t^e \sim \mathcal{N}(0, \sigma_\eta^2)$ and $\zeta_t^e \sim \mathcal{N}(0, \sigma_\zeta^2)$. The observation probability is denoted by $\mathbb{P}(\mathbf{z}_t|\mathbf{h}_t)$ and is given as below:

$$\begin{aligned} \mathbb{P}(\mathbf{z}_t|\mathbf{h}_t) &= \mathbb{P}(\tilde{\mathbf{V}}_t^{\mathcal{N}^o} | \mathbf{V}_t^{\mathcal{N}^o}) \mathbb{P}(\tilde{\boldsymbol{\theta}}_t^{\mathcal{N}^o} | \boldsymbol{\theta}_t^{\mathcal{N}^o}) \\ &\quad \mathbb{P}(\tilde{\mathbf{I}}_t^{\mathcal{E}^o} | \mathbf{I}_t^{\mathcal{E}^o}) \mathbb{P}(\tilde{\boldsymbol{\theta}}_t^{\mathcal{E}^o} | \boldsymbol{\theta}_t^{\mathcal{E}^o}). \end{aligned} \quad (12)$$

IV. LINE OUTAGE DETECTION ALGORITHM

In this section, we present our HMM-based dynamic algorithm for the line outage detection problem. We first formulate the problem as an inference problem and discuss how the standard forward-backward algorithm can be applied. Then we show that particle filtering can exploit the specific structure of the HMM in our setup to implement the inference algorithm.

A. Problem Formulation

Given an observed sequence $\mathcal{Z}_t = \{\mathbf{z}_1, \dots, \mathbf{z}_t\}$, the proposed algorithm generates a probability distribution $\pi_t(\mathbf{h})$ at each time slot t as an estimation of the hidden state $\mathbf{h}_t = (\mathbf{l}, \mathcal{S}_t)$:

$$\pi_t(\mathbf{h}) \equiv \mathbb{P}(\mathbf{h}_t = \mathbf{h} | \mathcal{Z}_t). \quad (13)$$

Note that the conditional distribution π_t gives the estimation of the line status at the current time slot t . The sequence of measurements also reveals more information about how the line status state evolved in the past, and this can potentially be used to backtrack the initial cause of the failures. In particular, based on the information filtration \mathcal{Z}_t , we can

update the previous estimation π_τ for all time slots $\tau < t$ to the conditional distribution $\pi_\tau^{(t)}$ as:

$$\pi_\tau^{(t)}(\mathbf{h}) \equiv \mathbb{P}(\mathbf{h}_\tau = \mathbf{h} | \mathcal{Z}_t). \quad (14)$$

Those probabilities can then be used as the input of more sophisticated fault diagnosis schemes. For example, threshold-based alarm schemes can build upon the marginal probability distribution of the line status \mathbf{l} and report the lines that are most likely to have failed.

$$\pi_t(\mathbf{l}) = \mathbb{E}[\pi_t(\mathbf{l}, \mathcal{S}) | \mathbf{l}] = \int_{\mathcal{S}} \pi_t(\mathbf{l}, \mathcal{S}) d\mathcal{S}, \quad (15)$$

Secondly, using the updated estimation $\{\pi_\tau^{(t)} : \tau \leq t\}$, it is possible to backtrack the entire realization path of the line failure cascades, identify the initial failure location, and take appropriate actions to recover the faulted lines. Following the Bayesian rules, the conditional probability can be written recursively as:

$$\pi_t(\mathbf{h}) \propto \mathbb{P}(\mathbf{z}_t | \mathbf{h}_t = \mathbf{h}) \int_{\mathbf{h}'} \mathbb{P}(\mathbf{h}_t = \mathbf{h} | \mathbf{h}_{t-1} = \mathbf{h}') \pi_{t-1}(\mathbf{h}'). \quad (16)$$

Similarly, for $\tau < t$,

$$\pi_\tau^{(t)}(\mathbf{h}) \propto \underbrace{\mathbb{P}(\mathbf{h}_\tau = \mathbf{h} | \mathcal{Z}_\tau)}_{\pi_\tau(\mathbf{h})} \underbrace{\mathbb{P}(\mathbf{h}_\tau = \mathbf{h} | \mathbf{z}_{\tau+1}, \dots, \mathbf{z}_t)}_{\rho_\tau^{(t)}(\mathbf{h})}, \quad (17)$$

where $\rho_\tau^{(t)}$ can be computed recursively by:

$$\begin{aligned} \rho_\tau^{(t)}(\mathbf{h}) & \\ \propto \int_{\mathbf{h}'} \mathbb{P}(\mathbf{h}_{\tau+1} = \mathbf{h}' | \mathbf{h}_\tau = \mathbf{h}) \mathbb{P}(\mathbf{z}_{\tau+1} | \mathbf{h}_{\tau+1} = \mathbf{h}') \rho_{\tau+1}^{(t)}(\mathbf{h}'). \end{aligned} \quad (18)$$

For notational convenience, in the above derivation we only considered the proportionality and ignored the multiplicative constant, which can be easily determined based on the normalization requirements.

B. Particle Filter Based Approximate Algorithm

Recall that the transition probabilities of the hidden states are sparse. Leveraging this property, we apply particle filtering to approximate the conditional distributions π_t and $\pi_\tau^{(t)}$, and only maintain a succinct representation of the conditional probabilities. Moreover, by choosing the number of particles, we are able to control the computation complexity.

The general principle of particle filter is to approximate a probability distribution using a set of P sample values and the associated importance weights. We denote the set of particles by $\{(\mathbf{h}_t^i, w_t^i) : i = 1, 2, \dots, P\}$, and the conditional probability π_t is approximated by:

$$\hat{\pi}_t(\mathbf{h}) = \sum_{i=1}^P w_t^i \delta_{\mathbf{h}_t^i}(\mathbf{h}), \quad \hat{\pi}_t(\mathbf{l}) = \sum_{i=1}^P w_t^i \delta_{\mathbf{l}_t^i}(\mathbf{l}), \quad (19)$$

where $\delta_{x_0}(x)$ is the Dirac function with the delta mass located at x_0 . Similarly, the approximation for $\pi_\tau^{(t)}$ is given by:

$$\hat{\pi}_\tau^{(t)}(\mathbf{h}) = \sum_{i=1}^P w_\tau^i \delta_{\mathbf{h}_\tau^i}(\mathbf{h}), \quad \hat{\pi}_\tau^{(t)}(\mathbf{l}) = \sum_{i=1}^P w_\tau^i \delta_{\mathbf{l}_\tau^i}(\mathbf{l}). \quad (20)$$

In Algorithm 1, we provide the basic flow of the particle filter based inference algorithm. It consists of two main steps at each time slot: resampling particles according to the likelihood of the particles, and updating the weights based on the instantaneous PMU readings. As the algorithm runs, some weights may become very small. In order to efficiently use the finite number of particles to represent the distributions, we need to occasionally resample the particles. We follow the rule of thumb to resample when the ratio $1/\sum_{i=1}^P (w_t^i)^2$ falls below a threshold $P/2$ [12]. The detailed steps are given in Algorithm 2.

Algorithm 1 Particle Filter Based Inference Algorithm

Input: Transition probabilities $\mathbb{P}(\mathbf{h}_{t+1}|\mathbf{h}_t)$, observation probabilities $\mathbb{P}(\mathbf{z}_t|\mathbf{h}_t)$, sequential observations $\{\mathbf{z}_t : t = 1, 2, \dots\}$

Output: Hidden system state probability estimation $\hat{\pi}_t(\mathbf{h}), \hat{\pi}_\tau^{(t)}(\mathbf{h}), (\tau < t)$

Initialization: at $t = 0$, draw particles from the stationary distribution: $\mathbf{h}_0^i \sim \mathbb{P}_0(\mathbf{h})$, set weight $w_0^i = \frac{1}{P}$

for $t = 1, 2, \dots$ **do**

for $i = 1, 2, \dots, P$ **do**

 Resample the particle according to (5):

$$\mathbf{h}_t^i \sim \mathbb{P}(\mathbf{h}_t|\mathbf{h}_{t-1}^i)$$

 Update the particle weight according to (12)

$$w_t^i = w_{t-1}^i \mathbb{P}(\mathbf{z}_t|\mathbf{h}_t^i)$$

 Optional Particle Management as in Algorithm 2

end for

$$\hat{\pi}_t(\mathbf{h}) = \sum_{i=1}^P w_t^i \delta_{\mathbf{h}_t^i}(\mathbf{h}), \quad \hat{\pi}_\tau^{(t)}(\mathbf{h}) = \sum_{i=1}^P w_t^i \delta_{\mathbf{h}_\tau^i}(\mathbf{h}).$$

end for

The following proposition provides the statistical consistency of the algorithm as the number of particles P goes to infinity.

Proposition 1: In Algorithm 1, for all t and τ , $\lim_{P \rightarrow \infty} \hat{\pi}_t(\mathbf{h}) = \pi_t(\mathbf{h})$, and $\lim_{P \rightarrow \infty} \hat{\pi}_\tau^{(t)}(\mathbf{h}) = \pi_\tau^{(t)}(\mathbf{h})$ almost surely.

Proof: It is a direct application of the convergence result of Theorem 1 in [13]. We omit the details due to the page limitations. ■

Algorithm 2 Particle Management

Input: Particles $\{(\mathbf{h}_{1:t}^i, w_t^i) : i = 1, \dots, P\}$

Output: New particles $\{(\mathbf{h}_{1:t}^i, \tilde{w}_t^i) : i = 1, \dots, P\}$

if $\frac{1}{\sum_{i=1}^P (w_t^i)^2} < \frac{P}{2}$ **then**

for $i = 1, 2, \dots, P$ **do**

 Sample an index j from a multinomial distribution

 with probabilities $p(j) = \frac{w_t^j}{\sum_{i=1}^P w_t^i}$

 Set $\tilde{\mathbf{h}}_{1:t}^i = \mathbf{h}_{1:t}^j$, and $\tilde{w}_t^i = \frac{1}{P}$

end for

end if

C. Complexity Analysis

Consider a frame of T time slots. Given the sequence of measurements $\mathcal{Z}_T = \{\mathbf{z}_1, \dots, \mathbf{z}_T\}$, By the end of the time frame T , the proposed algorithm computes the following estimation:

$$\mathbf{I}^{*(T)} \triangleq \left[\mathbf{I}_t^{*(T)} = \arg \max_{\mathbf{I}} \mathbb{E} \left[\pi_t^{(T)}(\mathbf{I}, \mathcal{S}) | \mathbf{I} \right] : t = 1, \dots, T \right]. \quad (21)$$

Over the T time slots, there are $\mathcal{O}(2^{ET})$ different realization paths that the evolution of the line status state can possibly take. Directly solving a multiway hypothesis testing problem involves computational complexity exponential in ET , and quickly becomes intractable as the size of the transmission network and/or the time frame increases. However, with the line failure model in (6), the cascading failure process only has a few realizations with high probabilities. This motivates us to implement the approximate algorithm with P particles for $P \ll \mathcal{O}(2^E)$. Then, the hypothesis testing is simplified into a probability estimation problem which can be efficiently and sequentially solved with the proposed algorithm.

The algorithm mainly consists of three parts: (1) resampling, (2) weight updating, (3) particle management (optional). Since given the power flow profile the lines fail with independent probabilities, for each particle we can execute the resampling step by sampling every line independently and in parallel. This dramatically reduces the computational complexity to the order of $\mathcal{O}(E)$. Moreover, we can parallel the updating step for the particles and speed up the overall inference algorithm. Let C denote the complexity of solving the AC power flow problem. Consequently, the total computational complexity of the algorithm is successfully reduced to $\mathcal{O}(TP(E+C))$.

V. CASE STUDY

A. Simulation Setting

We test the proposed HMM-based dynamic line outage detection algorithm on several IEEE standard testing systems: the 6-bus example from page 104–124 in [14], the 4-bus, 14-bus, 30-bus, 57-bus, 118-bus and 300-bus testing systems from [15].

AC Power Flow: To solve the AC power flow equations (3) – (4), we first specify the slack bus, PV buses and PQ buses. We solve the AC power flow equations using the Fast Decoupled method in Matpower with a tolerance level $1e^{-3}$. We ignore all the generator limits, the branch flow limits, and the voltage magnitude limits.

Failure model parameters: We adopt the functions $g_1(x) = \delta$ and $g_2(x) = 1 - e^{-\alpha x}$ for line failure probabilities in (6) with parameter $\delta = 0.02$ and $\alpha = 0.1$. We implement the proposed algorithm with the exact parameters ($\delta = 0.02, \alpha = 0.1$), and also with parameters with modeling error ($\delta = 0.025, \alpha = 0.2$). By comparing the two cases, we show that the proposed algorithm is robust to model parameter errors.

Adaptive power injection policy: The power injection profile is adjusted according to the topology change and is ruled by the following principles, which only aim to capture the basic features of the power injection policies.

- 1) disconnected components are removed from the system;
- 2) if the slack bus is disconnected from the system, a PV bus is chosen as the new slack bus;

- 3) if the original system breaks into several isolated parts, each part is operated separately with its own slack bus.

PMU observations: The PMU locations are optimized, and we normalize all the magnitude related readings to in the range $[0, 1]$, and all the phase related readings to in the range $[-\pi, \pi]$. The measurement noise is modeled as additive Gaussians to the normalized readings, and we set $\sigma_\epsilon = \sigma_\eta = \sigma_\zeta = \sigma_\eta = 0.15$ in (8)–(11). These parameters are also used to compute the observation probabilities in (12).

B. Simulation Result

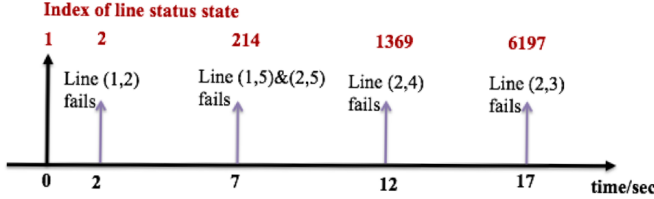


Fig. 1. A realization path of transmission line cascading failure. At time 7, there are two transmission lines outage occurring at the same time.

We use 1000 particles to approximate the conditional distribution the line status state $\pi_t(\mathbf{l}) \equiv \mathbb{P}(\mathbf{l}_t = \mathbf{l} | \mathcal{Z}_t)$, and computes the conditional distribution $\pi_t^{(T)}(\mathbf{l}) \equiv \mathbb{P}(\mathbf{h}_t = \mathbf{h} | \mathcal{Z}_T)$ at the end of the time frame $T = 20$. The conventional static algorithm computes the likelihood of the line status states $\mathbb{P}(\mathbf{l}_t | \mathbf{z}_t)$ using only the instantaneous observation \mathbf{z}_t .

Fig. 1 shows one specific line failure realization in the 14-bus system, and Fig. 2 and Fig. 3 compare the probabilistic estimates given by the proposed algorithm and the static algorithm. This example sheds light on why the proposed algorithm outperforms the conventional one, and we summarize the main observations below:

- 1) *Resilience to measurement noise:* The proposed algorithm is able to average the measurement noise over multiple time slots and yield a more accurate estimation.
- 2) *Eliminating ambiguous states:* With the limited number of PMUs, two different line status configuration can yield very close or even the same readings. For example, state 2, 38 and 39 yield instantaneous statistically indistinguishable PMU readings. When the true state is one of them, the static algorithm is not able to distinguish the three states, yet the proposed algorithm can correctly rule out the improbable states.
- 3) *Adaptive improvement:* The distribution π_t^T , which is based on measurements in the entire time frame, yields a better estimation over π_t . This shows that information accumulation over time facilitates identifying of the entire failure path.
- 4) *Robustness to modeling errors:* The proposed HMM-based inference method is robust to the modeling errors, as Fig. 2 and Fig. 3 show similar estimations when the algorithm is implemented with different model parameters.

We also study how the computational complexity scales with the size of the system and the number of particles. Fig. 4 compares the computational complexity between the static algorithm (execution time per iteration), and the HMM-based algorithm (average execution time of each particle per

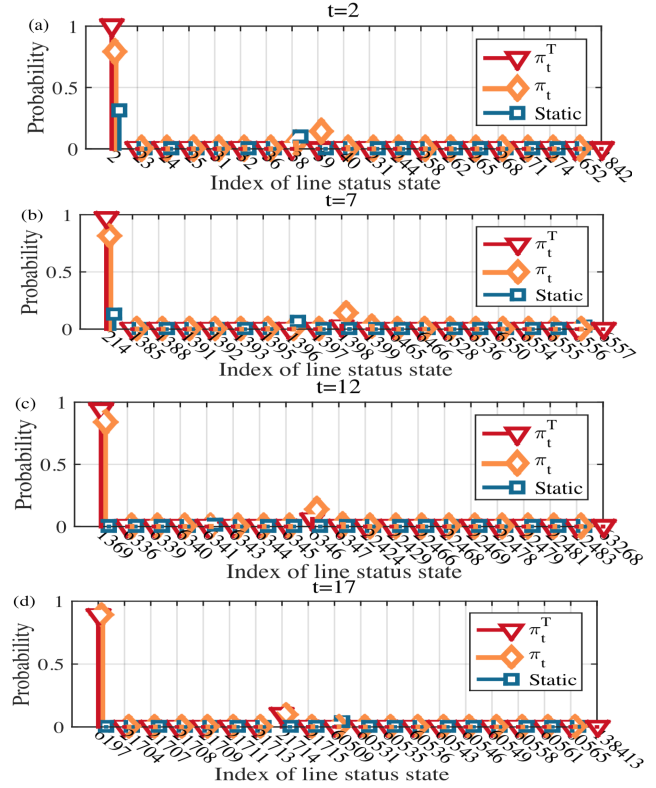


Fig. 2. We compare the estimations of the line status state over the time frame $T = 20$ given by: the static line outage detection algorithm, which computes the conditional distribution $\mathbb{P}(\mathbf{l}_t | \mathbf{z}_t)$; and the proposed HMM-based dynamic line outage detection algorithm, which computes the conditional distributions $\pi_t, \pi_t^{(T)}$. For each subfigure, only the 20 states with the highest probability are plotted. For the HMM-based algorithm, the exact line failure model parameters ($\delta = 0.02, \alpha = 0.1$) are used.

iteration). Moreover, Fig. 5 shows that the average execution time of each particle per iteration decreases with the number of particles. This is also due to the sparsity of the states transitions: many particles are identical and follow the same updating rules. On the other hand, Fig. 6 shows that by increasing the number of particles, we can achieve a better estimation accuracy of the line status state. We show that by tuning the number of particles P , the computational complexity and the estimation accuracy can be balanced.

C. Average Performance

For a realization in the time frame T and an estimation sequence $\mathbf{l}^{*(T)}$ for the actual hidden state $\mathbf{l}^{(T)}$, we define the accuracy of the estimator to be:

$$1 - \frac{\|\mathbf{l}^{*(T)} - \mathbf{l}^{(T)}\|_H}{T},$$

where $\|\cdot\|_H$ denotes the Hamming distance, which counts the number of positions at which the two sequences differ. We compare the accuracy of the three schemes: the static estimation

$$\mathbf{l}_{\text{static}}^{*(T)} \triangleq [\mathbf{l}_{t,\text{static}}^* = \arg \max \mathbb{P}(\mathbf{z}_t | \mathbf{l}) : t = 1, \dots, T],$$

the HMM-based estimation

$$\mathbf{l}_{\text{hmm real time}}^{*(T)} \triangleq [\mathbf{l}_{t,\text{hmm real time}}^* = \arg \max \pi_t(\mathbf{l}) : t = 1, \dots, T],$$

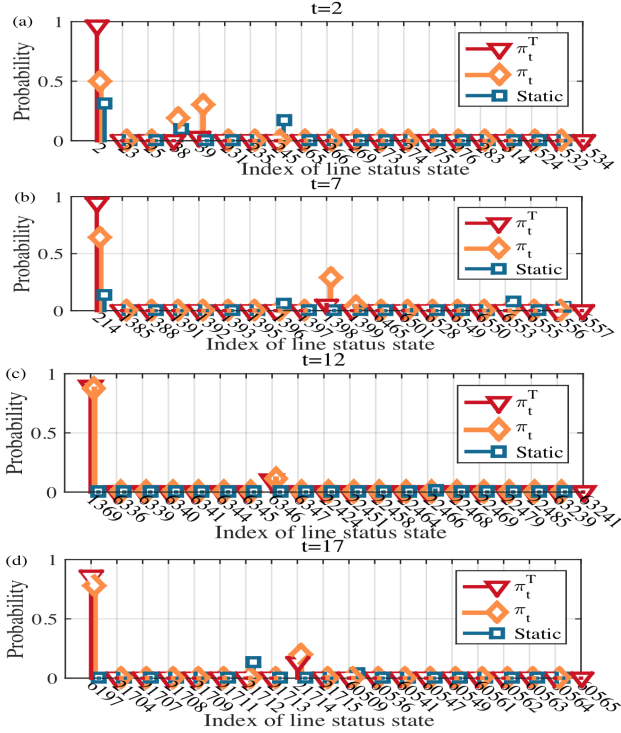


Fig. 3. Same setting as in Fig. 2, except for that the perturbed line failure model parameters ($\delta = 0.025, \alpha = 0.2$) are used in the HMM-based algorithm.

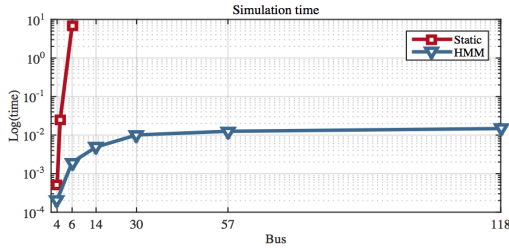


Fig. 4. Comparison between the execution time per iteration of the static algorithm and the average execution time per iteration for each particle of the HMM-based algorithm.

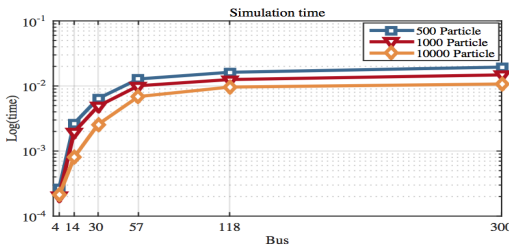


Fig. 5. Average execution time per particle per iteration for different number of particles.

and the HMM-based method

$$\mathbf{I}_{\text{hmm filtering}}^*(T) \triangleq \left[\mathbf{I}_{t, \text{hmm filtering}}^* = \arg \max \pi_t^{(T)}(\mathbf{l}) : t = 1, \dots, T \right].$$

We start all realization paths from state 1, i.e., all lines are in good condition, and terminate each realization path once it

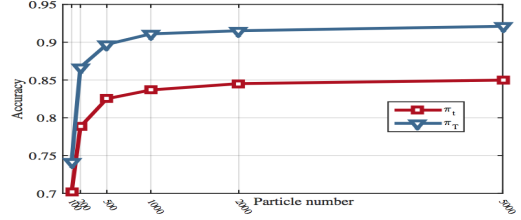


Fig. 6. Accuracy of the proposed algorithm on the 14 Bus case for different number of particles

reaches an absorbing state. Here a state is an absorbing state if there is no feasible power solution under the current power injection and network configuration. We simulated 2000 realization paths for three different levels of the measurement noise. The table in Fig. 7 compares the average performance of the three schemes, and we can see that the proposed algorithm significantly outperforms the static algorithm for every noise level.

Probability of correctness for different levels of measurement noise			
Noise level ϵ	0.1	0.15	0.2
Static	0.4094	0.3106	0.2231
HMM Real Time	0.909	0.789	0.687
HMM With Filter	0.9936	0.9588	0.9135

Fig. 7. Average performance of line status estimation given by the three algorithms. We choose three noise levels for $\sigma_\epsilon = \sigma_\epsilon = \sigma_\zeta = \sigma_\eta$ to be 0.1, 0.15 and 0.2. The HMM-based algorithms outperform the static algorithm for all noise levels.

REFERENCES

- [1] J. Chen and R. J. Patton, *Robust model-based fault diagnosis for dynamic systems*. Springer Publishing Company, Incorporated, 2012.
- [2] S. X. Ding, *Model-based fault diagnosis techniques*. Springer, 2008, vol. 2013.
- [3] I. Dobson, B. A. Carreras, V. E. Lynch, and D. E. Newman, “Complex systems analysis of series of blackouts: Cascading failure, critical points, and self-organization,” *Chaos: An Interdisciplinary Journal of Nonlinear Science*, vol. 17, no. 2, p. 026103, 2007.
- [4] G. Giannakis, V. Kekatos, N. Gatsis, S. Kim, H. Zhu, and B. Wollenberg, “Monitoring and optimization for power grids: A signal processing perspective,” *Signal Processing Magazine, IEEE*, vol. 30, no. 5, pp. 107–128, 2013.
- [5] W. Pan, Y. Yuan, H. Sandberg, J. Goncalves, and G.-B. Stan, “Real-time fault diagnosis for large-scale nonlinear power networks,” in *Decision and Control (CDC), 2013 IEEE 52nd Annual Conference on*, 2013, pp. 2340–2345.
- [6] V. V. Arthur R. Bergen, *Power Systems Analysis*. Prentice Hall, 2000, vol. 10.
- [7] O. Cappé, E. Moulines, and T. Rydén, *Inference in hidden Markov models*. Springer, 2005, vol. 6.
- [8] I. Dobson, D. Newman, B. Carreras, and V. Lynch, “An initial model for complex dynamics in electric power system blackouts,” in *2013 46th Hawaii International Conference on System Sciences*, vol. 2. IEEE Computer Society, 2011, pp. 2017–2017.
- [9] J. Chen, J. S. Thorp, and I. Dobson, “Cascading dynamics and mitigation assessment in power system disturbances via a hidden failure model,” *International Journal of Electrical Power & Energy Systems*, vol. 27, no. 4, pp. 318–326, 2005.
- [10] M. Anghel, K. A. Werley, and A. E. Motter, “Stochastic model for power grid dynamics,” in *System Sciences, 2007. HICSS 2007. 40th Annual Hawaii International Conference on*. IEEE, 2007, pp. 113–113.
- [11] Y. Weng, R. Negi, and M. D. Ilic, “Historical data-driven state estimation for electric power systems,” in *Smart Grid Communications (SmartGridComm), 2013 IEEE International Conference on*. IEEE, 2013, pp. 97–102.
- [12] B. Ristic, S. Arulampalam, and N. Gordon, *Beyond the Kalman filter: Particle filters for tracking applications*. Artech house, 2004.
- [13] D. Crisan and A. Doucet, “A survey of convergence results on particle filtering methods for practitioners,” *Signal Processing, IEEE Transactions on*, vol. 50, no. 3, pp. 736–746, 2002.
- [14] A. J. Wood and B. F. Wollenberg, *Power Generation, Operation, and Control, 2nd Edition*. John Wiley and Sons, NY, 1996.
- [15] , “IEEE power system test case archive, available at: <http://www.ee.washington.edu/research/pstca/>,” 2014.